Design and Measurements of Dual-Polarized Wideband Constant-Beamwidth Quadruple-Ridged Flared Horn

Ahmed Akgiray*, Sander Weinreb
Electrical Engineering
California Institute of Technology
Pasadena, CA, 91125, USA
Email: ahmed@caltech.edu

William Imbriale
Jet Propulsion Laboratory
California Institute of Technology
Pasadena, CA, 91109, USA

***Abstract*—A quad-ridged, flared horn achieving nearly constant beamwidth and excellent return loss over a 6:1 frequency bandwidth is presented. Radiation pattern measurements show excellent beamwidth stability from 2 to 12 GHz. Measured return loss is > 10 dB over the entire band and > 15 dB from 2.5 to 11 GHz. Using a custom physical optics code, system performance of a radio telescope is computed and predicted performance is average 70% aperture efficiency and 10 Kelvin of antenna noise temperature.**

Keywords-wideband horn; constant beamwidth horn; decade bandwidth; quad-ridge horn; profiled horn (key words)

I. INTRODUCTION

Increasing interest in wideband and continuous coverage radio astronomy necessitates development of wideband single-pixel feeds for future radio telescopes such as the Square Kilometer Array. These feeds must cover at least 5:1 (preferably > 10:1) frequency bandwidth over which return loss should be ≥ 10 dB and radiation pattern variation as a function of frequency must be minimized for best overall system efficiency [1]. Furthermore, radio telescope arrays with large number of dishes (a.k.a. large-N arrays) require that the feeds be easy to manufacture and maintain and be conducive to operation in a cryogenics dewar in order to minimize cost and maximize system sensitivity.

While there are multiple wideband feeds under consideration for radio telescopes such as the SKA ([2]-[4]), the quadruple-ridge flared horn described herein is unique in several respects. Its most distinct feature is the ability to design the horn to have a nearly constant beamwidth over a 6:1 frequency band for nominal 10 dB beamwidths between 60 and 130 degrees. Therefore, this horn could enable broadband frequency coverage on radio telescopes of different optical configurations and to the best knowledge of the authors, it is the only feed to accomplish this.

The horn presented here is not only capable of accommodating diverse antenna optics but also different input impedance requirements such antennas may present. The input impedance of this horn could be designed to have a nominal value between 50 and 100 Ohms while requiring only one single-ended low-noise amplifier (LNA) per polarization. The 50 Ohm input impedance is convenient for prototyping, testing and integration with other radio frequency components; however, a 100 Ohm design exhibits slightly better performance electrically and is more forgiving to mechanical tolerances. The all-metal and enclosed structure eliminates any impact a cryogenics dewar may have on feed performance and is easy to manufacture and maintain.

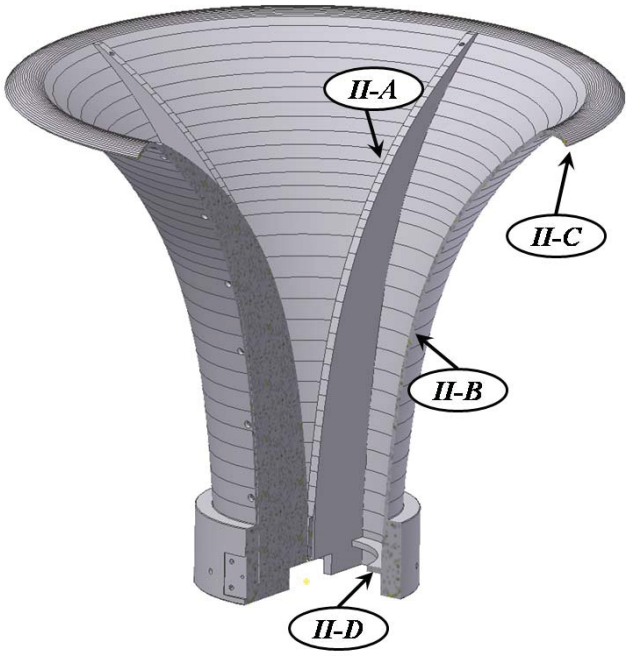

Figure 1. Three-quarter section view of the quad-ridged flared horn. Horn features are labeled according to subsection in which they are discussed.

An outline of this paper is as follows:

1) Design process and basics of operation,
2) Measured horn performance,
3) Predicted system performance on a radio telescope.

II. HORN DESIGN DETAILS

Ridged waveguides of constant waveguide and ridge cross-sections have been analyzed previously in the literature using magnetic field integral equations [5]-[6]. An equally thorough

theoretical analysis of ridged horns is notably lacking from the literature. On the other hand, there is ample information on profiled horn design both for smooth-walled and corrugated horns. The approach used in this work is to combine ideas of ridged waveguides, profiled and aperture-matched horns [7] and through use of CST Microwave Studio® (MWS) EM simulation software, empirically determine the horn configuration yielding desired performance. The following subsections describe details of the ridges, profiled walls, curved aperture and mode suppressor.

A. Ridges

Ridges serve two purposes in this design. First, they lower the cutoff frequency of the dominant waveguide mode by as much as factor of four thereby enabling single-mode operation over a large bandwidth [6]. The standard equation for cutoff frequency of TE modes in hollow circular waveguide, namely [8]

$$f_c = \frac{c}{2\pi}\frac{p'_{nm}}{a} \qquad (1)$$

where c is speed of light in free space, a is radius of circular waveguide and p'_{nm} is the mth zero of the derivative of the nth order Bessel function, suggests a TE_{11} mode cutoff frequency of approximately 3.21 GHz for guide radius of 27.395 millimeters (actual radius of horn in Fig. 1). On the other hand, cutoff frequency of the same guide including the ridges is computed by CST MWS to be 0.85 GHz. While dominant mode cutoff frequency is significantly lowered by the presence of ridges, ridge impact on cutoff frequencies of higher order modes, which can propagate in a four-fold symmetric structure, is much less pronounced.

While presence of ridges and their proximity to each other are the primary factors determining the single-mode bandwidth of the horn, ridge profile transforms the 50 Ohm input impedance to 377 Ohm free-space impedance at the horn aperture. As such, appropriate profile selection is paramount to obtaining good return loss performance. Various different profiles have been reported in literature, e.g. elliptical, exponential, linear, Gaussian, Fermi-like, some of which were evaluated as part of the design process. The best results have, so far, been achieved by the exponential profile which is the profile used in this work. It is a slightly simplified version of the profile reported in [9], namely

$$x = c_1\left(e^{Rz} - 1\right) \text{ where } c_1 = \frac{H/2}{e^{RL} - 1} \qquad (2)$$

The taper length and aperture diameter are given by L and H, respectively. The opening rate is determined by R. In general, a slower opening rate, implying a more slowly varying profile, yields better return loss performance.

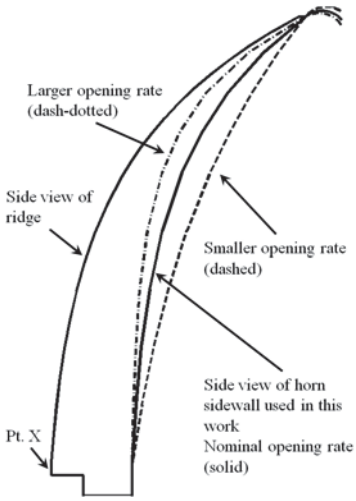

Figure 2: Cross-sectional view of the ridge and sidewall profiles used in this work. Also plotted are sidewall profiles with smaller (dashed) and larger (dash-dotted) opening rates. Signal is launched into the feed from point X.

B. Profiled Sidewall

Similar to the ridges, horn sidewall follows an exponential profile albeit with a different opening rate which is selected to strike a balance between two conflicting requirements. First, the horn should always be above cutoff for the lowest frequency of operation which favors an oversized horn. On the other hand, an unnecessarily oversized horn is prone to higher-order mode generation.

While a small opening rate (dashed line in Fig. 2) ensures operation well above cutoff throughout the length of the horn thereby yielding excellent return loss performance, it also decreases cutoff frequency of the higher order modes prohibitively. In addition, sidewall profile has a direct impact on aperture phase distribution (by way of changing path length to aperture) which is critical to obtaining near-constant beamwidth over a broad frequency range.

On the other hand, a horn sidewall with a larger opening rate (dash-dotted line in Fig. 2) cannot sustain propagation of the dominant TE_{11} mode above cutoff because as ridge-to-ridge distance increases (and horn inner radius remains essentially the same), the TE_{11} cutoff frequency quickly increases. It is because of this tradeoff that the measured return loss exhibits a 10 dB cross-over at approximately 1.9 GHz while the simulated cutoff frequency at Point X of Fig. 2 is 0.85 GHz.

C. Aperture matching

Aperture-matched horn concept was first described in detail in [7] as a way of reducing edge diffraction from aperture edges. Unlike corrugated horns where diffraction is reduced by nulling edge fields, an aperture-matched horn reduces edge diffraction by introducing curved surfaces to aperture edges such that the resulting junction is smooth [7].

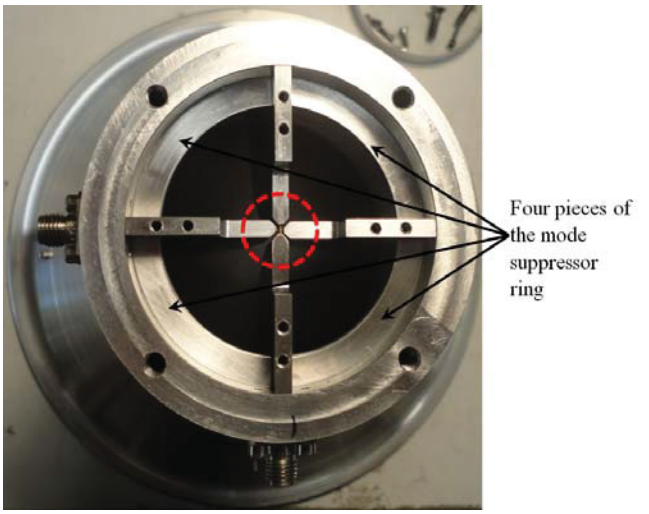

Figure 3. Photo of the bottom of the horn showing four pieces of the mode suppressor ring as well as the coax center conductor in the gap region.

In order not to increase size of the horn excessively, radius of curvature used in this work is approximately a tenth of the longest wavelength. According to [7], diffraction coefficient can further be decreased by making the radius of curvature at aperture edges on the order of half a wavelength. For this work, it was empirically observed that a smaller curvature of radius resulted in satisfactory reduction of far-out sidelobes as well as significant smoothing of the main beam.

D. Mode suppressor

It was reported in [6] that the first higher order mode that could be excited in a quadruple-ridged circular waveguide is the TE_{21L} mode, which is a result of mode splitting of the TE_{21} mode. We confirmed this with CST MWS simulations; however, it was also observed that excitation of TE_{12} mode is actually easier and more detrimental to overall performance. In particular, this mode has a strong electric field component aligned with that of TE_{11} in the gap region (whereas TE_{21L} electric field is zero in the same region). For frequencies where TE_{12} mode is above cutoff, it was observed that the coaxial probe used to excite TE_{11} mode also excited the TE_{12} mode with comparable amplitude. Excitation of this mode exhibited itself in horn radiation patterns as a sudden narrowing of the main beam in both E- and H-planes.

In order to avoid excitation of the TE_{12} mode, a mode suppressor is introduced around the launch point (see Fig. 3). Specifically, the mode suppressor is a metal ring with an inner radius ~30% smaller than sidewall radius. It is thin (approx. 3 millimeters) and thus is "invisible" at lower frequencies of operation and at the same time its radius is small enough to push cutoff frequency of TE_{12} mode to high end of the frequency band.

III. Measured Performance

A quad-ridged flared horn was built to verify simulation results as well as the design approach. The horn was designed to illuminate a 12-meter shaped dual-reflector antenna system, built by Patriot/Cobham, used in geodetic very long baseline interferometry (VLBI). Edge angle to the subreflector is 50 degrees. Thus, the horn was designed with a target 10 dB beamwidth of approximately 85 degrees. Measured return loss and radiation patterns are described in the next two subsections.

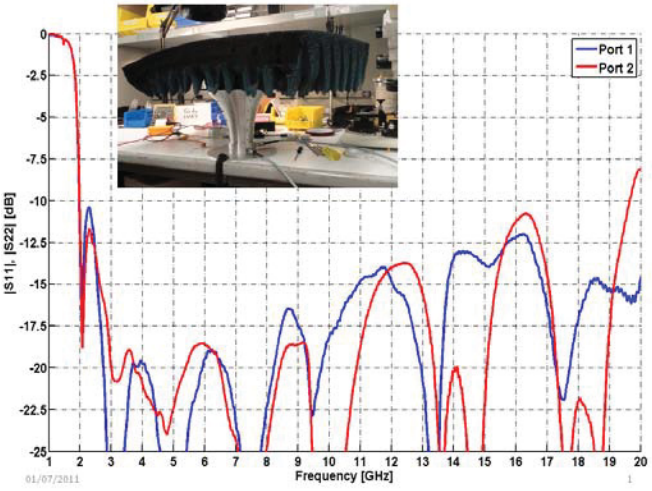

Figure 4. Photo of horn during return loss measurement (inset), and measured return loss for both polarizations.

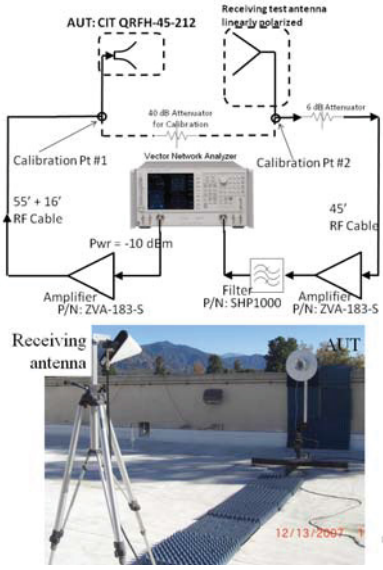

A. Return Loss

Due to single-ended nature of the horn design as well as its nominal 50 Ohm input impedance, it is very simple to measure return loss. Fig. 4 shows both a photo of the horn during return loss measurement and the measured performance. Measured return loss is higher than 10 dB from 1.9 GHz all the way up to 19 GHz. Furthermore, it is better than 15 dB from 2.5 to 11 GHz which is 85% of the target frequency band.

B. Radiation patterns

Horn radiation patterns were measured using a far-field pattern measurement setup on the roof of the electrical engineering building, Moore Laboratory, at Caltech. A block diagram of the test setup and a photo are shown in Fig. 6. Both

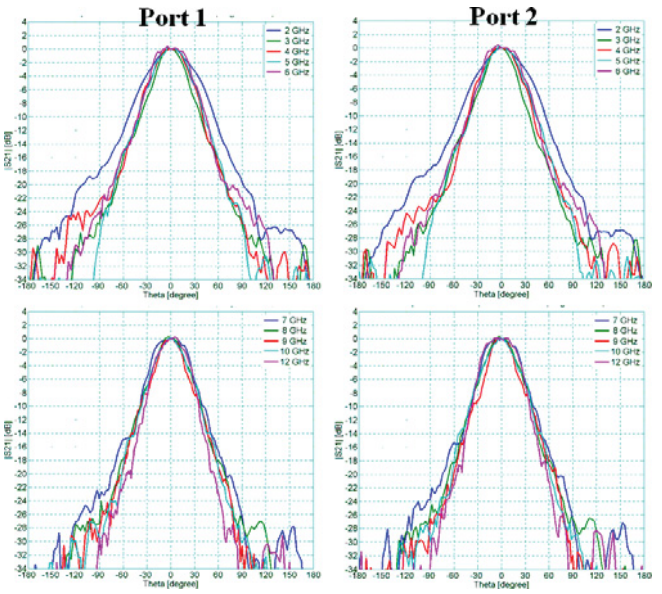

Figure 7. Measured co-polarized radiation patterns for Port 1 (left half), Port 2 (right half) in the ϕ = 45 degree plane.

co- and cross-polarized radiation patterns were measured in three azimuthal planes, namely ϕ = 0, 45, and 90 degrees, for θ = [-180, 180] degrees (with one degree steps in the main beam) from 1 to 17 GHz with a frequency resolution of 40 MHz.

Far-field patterns in the 45-degree plane are shown in Fig. 7 for both polarizations at 10 different frequencies. In excellent agreement with simulations, measurements show nearly constant beamwidth over the entire frequency band. Furthermore, any side or back lobes that may exist seem to be below the noise floor of our measurement setup which is around -25 to -30 dB. This suggests that spillover noise pickup of this horn should be minimal. The horn beamwidth is equally well-behaved in the 0-degree plane; however, it exhibits more variation in the 90-degree plane. This is expected due to the sinusoidal amplitude distribution of the dominant TE_{11} mode in this plane.

IV. Predicted System Performance

One of the most common figures-of-merit (FoM) used in radio astronomy to asses feed performance on a telescope is given by

$$FoM = \frac{A_{eff}}{T_{sys}}, \qquad (3)$$

where A_{eff} and T_{sys} are, respectively, the effective aperture area and system noise temperature. A physical optics program was used to compute the aperture efficiency of the 12-meter Patriot antenna taking into account shaping of both reflectors. The computed system aperture efficiency (not including dish, strut, losses) is plotted in Fig. 8. The predicted average aperture efficiency is over 69% over the entire band for both polarizations. Given the excellent measured return loss performance and very low feed loss predicted by CST MWS,

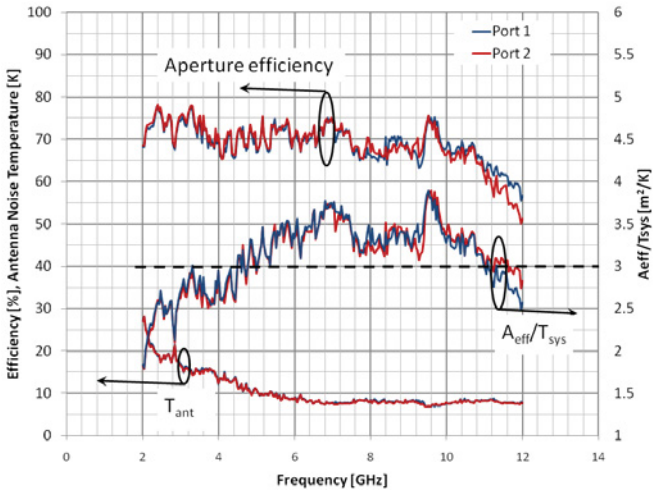

Figure 8. Aperture efficiency, antenna noise temperature and figure-of-merit calculations with this horn illuminating the 12-meter dual reflector system.

ohmic and mismatch losses in the feed should have a negligible impact on the actual aperture efficiency of this system.

Antenna temperature was calculated approximately for a zenith-pointing configuration using the method outlined in [10] and the result is shown in Fig. 8. It is less than 10 Kelvin over 70% of the band and its average from 2 to 12 GHz is 10 Kelvin. Assuming a 15 Kelvin receiver noise temperature, this yields the FoM curves plotted in Fig. 8 which suggest that the system performance is better than 60% efficiency and 23 K T_{sys} (black dashed line) for much of the band.

Acknowledgment

Part of the research was carried out at the Jet Propulsion Laboratory, California Institute of Technology, under a contract with the National Aeronautics and Space Administration.

References

[1] US SKA Consortium, "The Square Kilometer Array Preliminary Strawman Design Large N – Small D," SKA Memo #18, 2002.

[2] R. S. Gawande and R. F. Bradley, "Characterization of the active, inverted, conical sinuous antenna," XXIX General Assembly of URSI, Chicago, IL, Aug 2008.

[3] P-S. Kildal et al., "Development of a coolable 2-14 GHz Eleven feed for future radio telescopes for SKA and VLBI 2010," International Conference on Electromagnetics in Advanced Applications, pp. 545-547, 2009.

[4] G. Engargiola and W. J. Welch, "Log-periodic antenna," U.S. Patent 6 677 913, 2004.

[5] W. Sun and C. A. Balanis, "MFIE analysis and design of ridged waveguides," IEEE Trans. Microwave Theory Tech., vol. 41, pp. 1965-1971, Nov. 1993.

[6] W. Sun and C. A. Balanis, "Analysis and Design of Quadruple-Ridged Waveguides," IEEE Trans. Microwave Theory and Tech., vol. 42, pp. 2201-2207, Dec. 1994.

[7] W. D. Burnside and C. W. Chuang, "An Aperture-Matched Horn Design," IEEE Trans. Ant. Prop., vol. AP-30, no. 4, pp. 790-796, July 1982.

[8] N. Marcuvitz, Waveguide Handbook, MIT Radiation Laboratory Series, vol. 10, Lexington, MA: Boston Technical, 1964.

[9] J. Shin and D. H. Schaubert, "A parameter study of stripline-fed Vivaldi notch-antenna arrays," IEEE Trans. Ant. Prop., vol. 47, no. 5, May 1999.

[10] W. Imbriale, "Faster antenna noise temperature calculations using a novel approximation technique," IEEE Ant. Prop. Society International Symposium, pp. 1 – 4, Toronto, ON, July 2010.